Catalysis Science & Technology

Direct Epoxidation of Propylene with Water at PtOx Anode Using a Solid-Polymer-Electrolyte Electrolysis Cell

Journal:	*Catalysis Science & Technology*
Manuscript ID	CY-COM-10-2021-001888.R2
Article Type:	Communication
Date Submitted by the Author:	10-Dec-2021
Complete List of Authors:	Iguchi, Shoji; Tokyo Institute of Technology School of Materials and Chemical Technology , Department of Chemical Science and Engineering Kataoka, Masashi; Tokyo Institute of Technology School of Materials and Chemical Technology , Department of Chemical Science and Engineering Hoshino, Ryosuke; Tokyo Institute of Technology School of Materials and Chemical Technology , Department of Chemical Science and Engineering Yamanaka, Ichiro; Tokyo Institute of Technology School of Materials and Chemical Technology , Department of Chemical Science and Engineering

COMMUNICATION

Direct Epoxidation of Propylene with Water at PtO_x Anode Using a Solid-Polymer-Electrolyte Electrolysis Cell

Received 00th January 20xx,
Accepted 00th January 20xx

DOI: 10.1039/x0xx00000x

Shoji Iguchi,[a] Masashi Kataoka,[a] Ryosuke Hoshino [a] and Ichiro Yamanaka [a]*

Direct electro-epoxidation of C_3H_6 with water was achieved using a solid polymer electrolyte (SPE) electrolysis cell. PtO_x anode produced propylene oxide (PO) at a formation rate of 37 μmol h^{-1} cm^{-2} with a faradic efficiency of 7.4% by applying potential of 1.60 V (SHE) to the anode. Characterisation studies successfully revelaed that Pt oxide species (Pt(II) and Pt(IV)) are strongly related to the catalysis for the electro-epoxidation of C_3H_6. It is speculated that active oxygen species on the Pt oxide derived from water exihibits impressive activity for the PO production.

Propylene oxide (PO) is one of the most important intermediate raw materials for the petrochemical industry, therefore over 10 million ton of PO is produced per year around the world.[1] PO is commercially produced by chlorohydrin process, PO/styrene co-production process, PO/tert-butyl co-production process, Sumitomo cumene-based process, etc.[2] These indirect processes for the PO production are now operated to meet the huge demand, however there are some disadvantages such as risk of explosion of the peroxides, environmental destruction by harmful by-products, and complicated multi-steps. Recently, a new process for the PO production using H_2O_2 oxidant and the titanium silicate-1 (TS-1) catalyst has been developed.[3,4] At a laboratory level, investigations on simple oxidation of C_3H_6 with molecular O_2 have been studied over this half century. Ag-based catalysts, which are known as an excellent catalyst for ethylene oxidation to ethylene oxide, are also active for the PO production by adding the qualified additives.[5] Furthermore, TS-1 supported nano Au cluster catalyst enables the selective PO production with O_2 and H_2.[6,7] To achieve the sustainable development based on a carbon neutral society, it is essential to utilize renewable energy sources in the industrial scenes. Therefore, it is greatly desired to develop the photocatalysis or electrocatalysis for the direct epoxidation of C_3H_6. Whereas photocatalytic epoxidation of C_3H_6 with O_2 has been already demonstrated by using V_2O_5/SiO_2 photocatalyst,[8] number of reports focused on the electrolysis for propylene epoxidation are limited. Here, we report electro-epoxidation of C_3H_6 by using solid polymer electrolyte (SPE) electrolysis cell. The SPE is commonly used in the fuel cell and the water electrolysis.[9-11] Langer and Ogumi pioneered the chemical conversion of organic substrates using the SPE electrolysis,[12,13] and applied it to Kolbe electrolysis,[14] electro-oxidations,[15] electrohydrogenations,[16] etc. We have been also reported kinds of electrocatalytic reactions using the SPE electrolysis such as

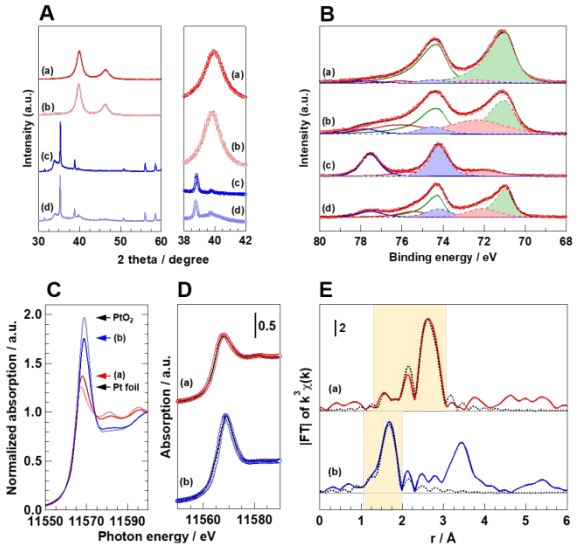

Figure 1. (A) XRD patterns and (B) Pt 4f XPS of (a) Pt black, (b) $PtO_x(O_2)$, (c) PtO_2, and (d) $PtO_x(N_2H_4)$. Pt L_3-edge (C) XANES spectra, (D) results of LCF analysis, and (E) FT-EXAFS spectra of (a) $PtO_x(O_2)$ and (b) $PtO_x(N_2H_4)$. Those of Pt foil and PtO_2 are also shown in (C). Circle plots and solid lines in (D) are original spectra and fitting results of LCF. Fitting range and fitting results of curve fitting analysis are presented in (E) by yellow back-colored and dashed lines, respectively.

[a] *Department of Chemical Science and Engineering, Tokyo Institute of Technology, Ookayama 2-12-1-S1-16, Meguro, Tokyo 152-8552, Japan*
Tel: +81−3−5734−2144. E-mail: yamanaka.i.aa@m.titech.ac.jp

† Electronic Supplementary Information (ESI) available: Schematic diagram of SPE electrolysis cell, summary of characterization results (bulk and surface) for the prepared anode catalysts and their PO production activities, and the experimental details of catalyst preparation, electrochemical activity test, and characterizations. See DOI: 10.1039/x0xx00000x

methanol oxidation,[17] H_2O_2 production,[18] CO_2 reduction,[19] and toluene hydrogenation.[20] On the other hand, our previous investigations revealed that C_3H_6 and 1-hexene were effectively oxidized to PO and 1,2-epoxy-5-hexene, respectively, by using Pt black anode incorporated in the electrolysis cell equipped with H_3PO_4 dipped-wool electrolyte, which is inspired by the SPE electrolysis.[21,22] With a view toward improving PO yield, it is strongly desired to apply the SPE electrolysis cell with Nafion membrane, which enables more prominent proton conductivity, higher durability and mechanical strength, to the oxidation of C_3H_6. It can be considered that active oxygen species (O*) derived from water activation at the anode should act as a strong oxidation reagent to give PO production under mild conditions.

In this study, electro-epoxidation of C_3H_6 to PO, acetone, and CO_2 with water was investigated by using the SPE electrolysis cell equipped with the handmade membrane-electrode-assembly (MEA, consisting of PtO_x anode, Nafion membrane, and Pt/C cathode), as shown in Figure S1. Purposes of this work are to confirm steadily progress of the electro-epoxidation of C_3H_6 with water by the SPE electrolysis cell, to clarify the effect of anode potential on the oxidation of C_3H_6, to reveal a correlation between the epoxidation activity and the oxidation state of the PtO_x anode, and to propose the reaction mechanisms based on characterization studies.

It was found that both partially oxidized Pt black with O_2 ($PtO_x(O_2)$) and partially reduced PtO_2 with N_2H_4 ($PtO_x(N_2H_4)$) are active anode catalysts for the electro-epoxidation of C_3H_6, as described in the latter part (see Supporting Information for the detailed catalyst preparation method). Therefore, characteristics of these catalysts were investigated by X-ray diffraction (XRD), X-ray photoelectron spectroscopy (XPS), X-ray absorption spectroscopy (XAS), and temperature programmed desorption (TPD) techniques. Both the Pt black and the prepared $PtO_x(O_2)$ showed typical XRD patterns corresponding to fcc-Pt crystal structure (Figure 1A). Changes in crystallinity by the oxidation treatment were not observed. On the other hand, $PtO_x(N_2H_4)$ exhibited diffraction patterns originated from Pt_3O_4 phase (Figure 1A). Broad diffraction peak at 39.65°, corresponded to fcc-Pt, was slightly appeared in the pattern of $PtO_x(N_2H_4)$. Wave deconvolution analysis of Pt $4f_{7/2}$ (dotted line) and $4f_{5/2}$ (solid line) XPS spectra revealed that Pt(II) component (red) was formed on the surface of both $PtO_x(O_2)$ and $PtO_x(N_2H_4)$ catalysts in addition to Pt(0) (green) and Pt(IV) (blue) components (Figure 1B). Averaged surface oxidation state of $PtO_x(O_2)$ and $PtO_x(N_2H_4)$ were estimated to 1.03 and 1.08, respectively, with respect to these composition ratios (Table S1). Pt L_3-edge XANES spectrum is also useful technique to evaluate the average oxidation state of bulk structure due to strong correlation between the white-line intensity and occupation of the Pt 5d orbital. Linear combination fitting (LCF) analysis of the XANES region using both PtO_2 and Pt foil as references provided that averaged oxidation state of $PtO_x(O_2)$ and $PtO_x(N_2H_4)$ bulk structure are 0.48 and 2.96, respectively (Figure 1C and D, Table S2. Normalized raw spectra can be found in Figure S2). Moreover, curve fitting analysis for 1st shell of FT-EXAFS spectra revealed that a slight Pt-O bonding (coordination number: 0.20, bond length: 1.98 Å) was confirmed in $PtO_x(O_2)$ catalyst, while fcc-Pt structure was maintained through the oxidation treatment (Figure 1E, Table S2). Furthermore, averaged oxidation state of $PtO_x(O_2)$ bulk structure was directly estimated by the amount of desorbed O_2 in the temperature programmed desorption experiments. Clear desorption peak with a peak top at 640 K was appeared by heating in He stream, which is originated from decomposition of PtO_x species to provide Pt metal (Figure 2A). As compared to the

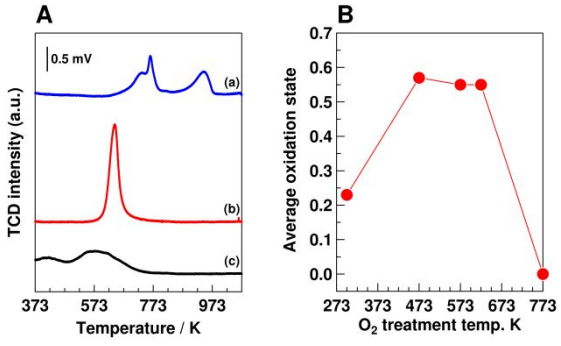

Figure 2. (A) Temperature programmed desorption profiles of (a) PtO_2, (b) $PtO_x(O_2)$, and (c) Pt black. (B) Averaged oxidation state of bulk structure of $PtO_x(O_2)$ prepared by the oxidation treatment of Pt black with 20% O_2 at various treatment temperatures calculated from TPD profiles.

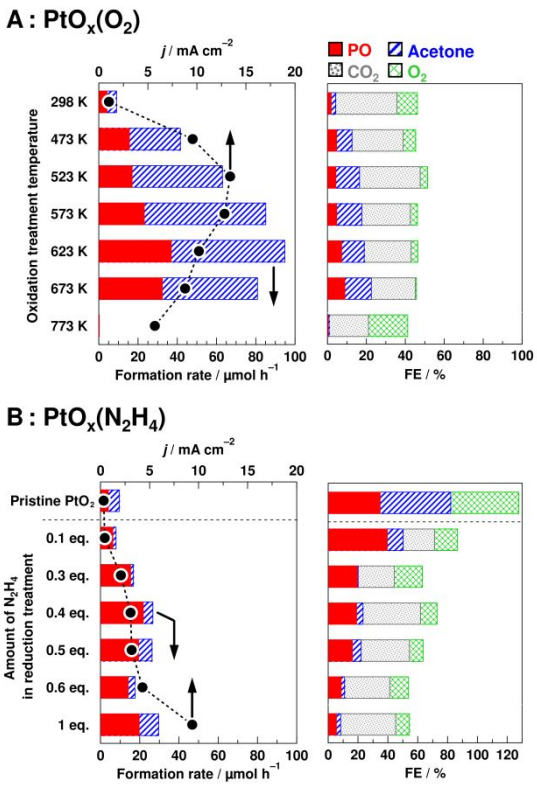

Figure 3. Averaged current density (*j*), formation rates and faradic efficiencies of products in the potentiostatic electrolysis at +1.60 V (SHE) using (A) $PtO_x(O_2)$ prepared by the oxidation of Pt black with 20%O_2 at various treatment temperatures, and (B) $PtO_x(N_2H_4)$ prepared by the reduction of PtO_2 with various concentration of N_2H_4 solution. $p(C_3H_6)$ were 1.0 atm and 0.33 atm for (A) and (B), respectively.

decomposition of rigid PtO_2,[23] $PtO_x(O_2)$ could be easily reduced at lower temperature, indicating that unstable PtO_x species is formed by the mild oxidation with20%O_2. Averaged oxidation state calculated from TPD experiments were obviously altered by O_2 treatment temperature in the oxidation process of Pt black (Figure 2B, Figure S3). These averaged oxidation state of $PtO_x(O_2)$ bulk structure are good agreement with those that are based on LCF analysis of XANES spectra. However, surface averaged oxidation state of $PtO_x(O_2)$ confirmed by XPS measurement was much higher than that of bulk structure (Table S1). From the results of characterisations for bulk structure (TPD, XANES and EXAFS) and surface composition (XPS), it can be speculated that Pt oxide species, which is concentrated on the surface of $PtO_x(O_2)$ catalyst, covers the Pt black core.[24]

Figure 3A displays results for the electro-epoxidation of C_3H_6 on $PtO_x(O_2)$ anodes at +1.60 V (SHE) conducted by using the SPE electrolysis cell. Average current density (*j*) was obviously increased by the O_2 oxidation at 473K, and reached to maximum at 523 K. Then, further oxidation treatment at higher temperature caused decreasing of *j*. Formation rate of PO was clearly increased by the oxidation treatment at 473K, and gradually accelerated with increases in the oxidation temperatures until 673 K. To be note, electrocatalysis for the PO formation was thoroughly disappeared by the oxidation treatment at 773 K. The formation rates of acetone exhibited similar trend to that of the PO formation. Faradic efficiencies (FE) of PO and acetone were gradually increased with the oxidation treatment temperature until 673K, while that of CO_2 was gradually decreased. FE of O_2 was quite low regardless of the oxidation treatment temperature, excepting for 773 K. Critical changes in the electrocatalytic activity were observed by the oxidation treatment at 773 K, which resulted in thoroughly reduced Pt black as shown in Figure 2B, suggested that the O_2 oxidation treatment at severe temperature do not generate the active site on the surface of Pt black. On the other hand, the reduction method using N_2H_4 as a reductant was also applied to the preparation of $PtO_x(N_2H_4)$ anode from commercial PtO_2 (see Supporting Information for detailed preparation procedures). Partially reduced $PtO_x(N_2H_4)$, as shown in Figure 3B, was found to be active for the electro-epoxidation of C_3H_6. Both *j* and the formation rate of PO were also elevated by the reduction of PtO_2 with N_2H_4. The formation rate of PO was increased with the increase of the amount of N_2H_4 used in the reduction treatment of PtO_2, whereas that of acetone formation was not improved. The formation of Pt(0) on the surface of PtO_2 by N_2H_4 reduction would result in the decrease in FE of PO. Pristine PtO_2 also exhibited certain activity for the electro-oxidation of C_3H_6, and PO and acetone were produced with FE of 35% and 47%, respectively. The reason why total FE for pristine PtO_2 was over 100% might be due to the decomposition of PtO_x species during the electrolysis. Accordingly, it was found that both the oxidized Pt black ($PtO_x(O_2)$) and the reduced PtO_2 ($PtO_x(N_2H_4)$), which have incomplete oxidation state, are active for the electro-epoxidation of C_3H_6.

As shown in Table S3, reproducibility of electro-epoxidation of C_3H_6 using the $PtO_x(O_2)$ anode demonstrated in the present work was sufficiently ensured. Figure S4 shows time courses of *j*, yield, and FE of products in the electro-epoxidation of C_3H_6 at +1.60 V (SHE) using the $PtO_x(O_2)$ anode. It was confirmed that the SPE electrolysis cell composed of homemade MEA enables to achieve a steady electrolysis, while *j* was gradually decreased. Yields of PO and acetone monotonically increased with the electrolysis time. The FEs of PO and acetone were almost constant with the electrolysis time, indicating that PO and acetone were concurrently produced from C_3H_6. The turnover number, Pt(TON), for the PO formation were calculated to 1.7 per surface exposed Pt atoms (see Supporting Information for the details), suggesting that Pt species functions as a catalyst for the electro-epoxidation of C_3H_6. Then, effect of anode potential on the electro-epoxidation of C_3H_6 at the $PtO_x(O_2)$ anode, prepared by 20%O_2 treatment at 623 K, was investigated, as shown in Figure 4. *j* and formation rates of PO and acetone were accelerated by increasing the anode potential. The larger FE of PO was observed at higher anode potentials, while that of acetone was slightly decreased with increase in the anode potential. Interestingly, certain amounts of PO, acetone, and CO_2 were produced even at +1.20 V (SHE), indicating that the C_3H_6 oxidation could be proceeded when the anode potential was less than the standard potential for H_2O oxidation (= +1.23 V (SHE), $O_2 + 4H^+ + 4e^- \rightarrow 2H_2O$). It can be said that molecular O_2 originated from water oxidation is not the required oxidant for the oxidation of C_3H_6 to PO using the SPE electrolysis. Moreover, the formation rate of O_2 confirmed at +1.60 V (SHE) was very low nevertheless that could give enough over potential for the H_2O oxidation to O_2, whereas O_2 was evolved with FE of approx. 100% in a control experiment with the absence of both C_3H_6 gas and CH_2Cl_2 solvent.

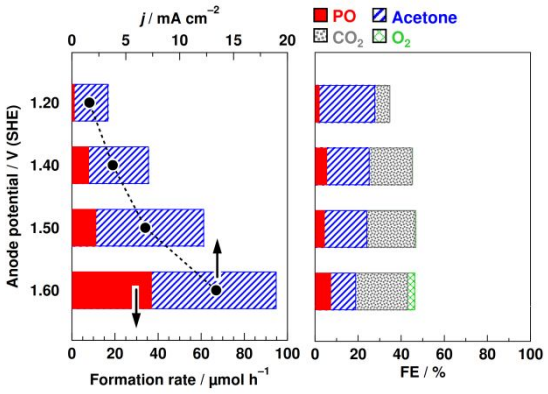

Figure 4. Averaged current density (*j*), formation rates and faradic efficiencies of products in the potentiostatic electrolysis at various anode potentials using $PtO_x(O_2)$ prepared by O_2 treatment at 623 K.

Figure 5 summarizes a correlation between the formation rates of PO and acetone at +1.60 V (SHE) and the surface composition of a series of $PtO_x(O_2)$. It can be clearly found that the increase of Pt(0) content gives drastic degradation of PO formation, while PtO_x catalysts with high Pt(0) content have good electron conductivity. On the other hand, the formation rate of PO was obviously enhanced with the increase of Pt(II) or Pt(IV) components, indicating that the surface Pt oxides species are essential for PO production. In addition to the strong

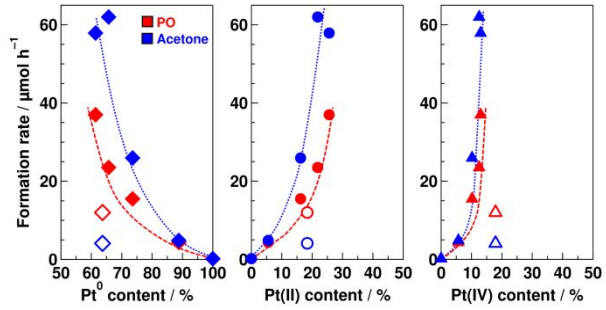

Figure 5. Correlation between formation rates of PO and acetone in the potentiostatic electrolysis at +1.60 V (SHE) and the surface components ratios of $PtO_x(O_2)$ evaluated by XPS analysis. Filled plots: a series of $PtO_x(O_2)$ catalysts, outlined plots: $PtO_x(N_2H_4)$ catalyst.

interaction between Pt oxide species and electrophobic double bond of C_3H_6, Pt oxide species would promote the water activation which forms the active oxygen species O*, those effectively activate C_3H_6 under mild conditions. Furthermore, the results of $PtO_x(N_2H_4)$ (outlined plots in Figure 5) showed good agreement with the trend of a PO yield for a series of $PtO_x(O_2)$. However, acetone production activity of $PtO_x(N_2H_4)$ was much lower than that of $PtO_x(O_2)$ regardless of its component ratio. Herein, we briefly propose the reaction mechanism as below. Pt oxide species such as Pt(II) and Pt(IV) formed on the surface of PtO_x anode are suited for water activation, and O* might be produced under moderate anode potential. C_3H_6 molecule adsorbed on the Pt oxide sites easily reacts with O* to result in the PO production. It can be estimated that Pt(II) also contributes to acetone formation with Wacker-type reaction. O_2 evolution caused by coupling of two active oxygen species is not to be preferential at the anode potential of +1.60 V (SHE); the majority of O* would be effectively utilized to oxidize C_3H_6. In summary, we successfully achieved direct electro-epoxidation of C_3H_6 using the SPE electrolysis cell incorporating the PtO_x anode, which provides active oxygen species through the electrochemical water activation. Although conversion rate of C_3H_6 and selectivity for PO are still now insufficient than previously reported superior catalytic system (Table S4), further development in electro-epoxidation of C_3H_6 is strongly expected by considering advantages such as (1) PO production can proceed at room temperature, and (2) easy handling due to applying non-mixtured feeding gas (co-presence of O_2 is unnecessary).

Conclusions

A first report on propylene oxide (PO) production in the electro-epoxidation of C_3H_6 with water using the SPE electrolysis cell is provided. Formation of PO, acetone, and CO_2 were accelerated by the catalysis of PtO_x anode, while O_2 formation was not. PO production was increased tenfold by mild oxidation of Pt black with 20% O_2 at 623 K. Characterisations clarified that Pt oxide species (Pt(II) and Pt(IV)), which covers Pt black core, is essential for the electro-epoxidation of C_3H_6 to PO. It is considered that the active oxygen species at PtO_x surface, derived from water, acts as an effective oxidant for selective C_3H_6 oxidation.

Conflicts of interest

There are no conflicts to declare.

Acknowledgment

This work was supported by JST-CREST projects (Grant Number JPMJCR18R1), Innovation in chemical reactions through active control of electrons and ions for production, by the Japan Ministry of Education, Culture, Sports, Science and Technology (MEXT). Pt L_3-edge XAFS measurement was performed at BL-9C of the photon factory (Japan) with approval of High Energy Accelerator Research Organization (experiment proposal No. 2019G629).

References

1 J. Y. Tomonori KAWABATA, Hirofumi KOIKE, Shuhei YOSHIDA, *SUMITOMO KAGAKU*, 2019, **2019-I**, 1.
2 S. J. Khatib and S. T. Oyama, *Catalysis Reviews*, 2015, **57**, 306-344.
3 V. Russo, R. Tesser, E. Santacesaria and M. Di Serio, *Industrial & Engineering Chemistry Research*, 2013, **52**, 1168-1178.
4 D. M. Perez Ferrandez, M. H. J. M. de Croon, J. C. Schouten and T. A. Nijhuis, *Industrial & Engineering Chemistry Research*, 2013, **52**, 10126-10132.
5 J. Rouchaud and M. De Pauw, *Journal of Catalysis*, 1969, **14**, 114-117.
6 J. Huang, T. Takei, T. Akita, H. Ohashi and M. Haruta, *Applied Catalysis B: Environmental*, 2010, **95**, 430-438.
7 J. Chen, S. J. A. Halin, E. A. Pidko, M. W. G. M. Verhoeven, D. M. P. Ferrandez, E. J. M. Hensen, J. C. Schouten and T. A. Nijhuis, *ChemCatChem*, 2013, **5**, 467-478.
8 F. Amano and T. Tanaka, *Catalysis Communications*, 2005, **6**, 269-273.
9 P. W. T. Lu and S. Srinivasan, *Journal of Applied Electrochemistry*, 1979, **9**, 269-283.
10 B. Smitha, S. Sridhar and A. A. Khan, *Journal of Membrane Science*, 2005, **259**, 10-26.
11 S. Shiva Kumar and V. Himabindu, *Materials Science for Energy Technologies*, 2019, **2**, 442-454.
12 S. H. Langer and S. Yurchak, *Journal of The Electrochemical Society*, 1969, **116**, 1228.
13 Z. Ogumi, S. Yoshizawa, *Denki-Kagaku (J. Electrochem. Soc. Japan)*, 1981, **49**, 212.
14 Z. Ogumi, H. Yamashita, K. Nishio, Z.-I. Takehara and S. Yoshizawa, *Electrochimica Acta*, 1983, **28**, 1687-1693.
15 Z. Ogumi, S. Ohashi and Z. Takehara, *Electrochimica Acta*, 1985, **30**, 121-124.
16 Z. Ogumi, K. Nishio and S. Yoshizawa, *Electrochimica Acta*, 1981, **26**, 1779-1782.
17 R. Kishi, H. Ogihara, M. Yoshida-Hirahara, K. Shibanuma, I. Yamanaka and H. Kurokawa, *ACS Sustainable Chemistry & Engineering*, 2020, **8**, 11532-11540.
18 I. Yamanaka and T. Murayama, *Angewandte Chemie International Edition*, 2008, **47**, 1900-1902.
19 H. Ogihara, T. Maezuru, Y. Ogishima, Y. Inami, M. Saito, S. Iguchi and I. Yamanaka, *ACS Omega*, 2020, **5**, 19453-19463.
20 Y. Inami, S. Iguchi, S. Nagamatsu, K. Asakura and I. Yamanaka, *ACS Omega*, 2020, **5**, 1221-1228.
21 K. Otsuka, T. Ushiyama, I. Yamanaka and K. Ebitani, *Journal of Catalysis*, 1995, **157**, 450-460.
22 I. Yamanaka, *Electrochemical and Solid-State Letters*, 1999, **2**, 131.
23 W. P. N. Seriani, L. C. Ciacchi, *The Journal of Physical Chemistry*, 2006, **110**, 14860.
24 D.C. Koningsberger, D.E. Sayers, *Slid State Ionics*, 1985, **16**, 23.